Thermochimica Acta 497 (2010) 137–142

Contents lists available at ScienceDirect

Thermochimica Acta

journal homepage: www.elsevier.com/locate/tca

Impact of synthesis conditions on surface chemistry and structure of carbide-derived carbons

Cristelle Portet[a], Dmitry Kazachkin[b,c], Sebastian Osswald[a,1], Yury Gogotsi[a,*], Eric Borguet[b]

[a] Department of Materials Science and Engineering, Drexel University, 3141 Chestnut Street, Philadelphia, PA 19104, USA
[b] Department of Chemistry, Temple University, Philadelphia, PA 19122, USA
[c] Department of Chemical Engineering, University of Pittsburgh, Pittsburgh, PA 15261, USA

ARTICLE INFO

Article history:
Received 13 February 2009
Received in revised form 26 July 2009
Accepted 9 September 2009
Available online 16 September 2009

Keywords:
Carbide-derived carbons (CDCs)
Temperature programmed desorption (TPD)
Chlorination
Surface chemistry
Porous carbon

ABSTRACT

Carbide-derived carbons produced by chlorination of titanium carbide at 600, 800, or 1100 °C were subjected to a post-treatment at 600 °C in Ar, H_2, or NH_3 atmosphere. Experimental results suggest that the chlorination temperature influences the ordering of carbon in a manner that impacts specific surface area and porosity. Higher chlorination temperatures lead to higher total pore volume and increased ordering, but lower microporosity. The effect of post-treatments on surface chemistry is pronounced only for samples chlorinated at 600 °C; post-treatments in Ar are shown to be less effective for chlorine removal than those performed in H_2 or NH_3. Post-treatments in Ar result in a lower total pore volume compared to the ones in H_2 or NH_3 for the same chlorination temperature. Samples chlorinated at higher temperatures contained less oxygen functionalities than samples chlorinated at 600 °C, and showed correspondingly less desorption of H_2O, possibly due to diminished uptake of ambient water.

1. Introduction

Porous carbon materials are widely used for filtration, purification, energy storage, and fabrication of biomedical systems [1]. One of the advantages of carbide-derived carbons (CDC) over conventional activated carbons is the ability to tune the porous structure with a very high accuracy [2–4]. That is due to a regular spacing between carbon atoms in the carbide lattice, which enables a narrow pore size distribution, large number of carbide precursors available for CDC synthesis, as well as a diversity of synthesis and processing conditions (e.g., temperature, chlorination time, etc.) that can be used to further control porosity. In particular, carbons derived from titanium carbide (TiC) have not only demonstrated a record-breaking performance in a variety of energy-related applications [3,4], but also enabled systematic studies of the effect of pore size on properties, which could not be performed on activated or other porous carbons. This led to improved understanding of ion adsorption in pores smaller than the solvated ion size [3] and other important scientific breakthroughs.

CDC synthesis from metal carbides is a multi-step process. The key step is metal extraction from the carbide lattice via chlorination at elevated temperatures with Cl_2 [4,5]. After chlorination, chlorine may be retained on the surface of the carbon having a negative effect on the performance of energy storage and biomedical devices, where pure carbon materials are required [6,7]. Therefore, it is important to eliminate residual chlorine from CDCs and post-treatments in Ar, NH_3 or H_2 were suggested for this purpose [8].

It was previously shown that the surface properties of carbon black and activated carbons chlorinated at moderate temperatures are modified due to chlorine bonded to the carbon surface [8,9]. The effect of synthesis conditions on porosity were mentioned in Refs. [8,9]. In the present paper, we studied the influence of chlorination and post-treatment conditions on the surface chemistry of CDC, the porosity of CDC, and the structure (ordering) of CDC, topics that have not been investigated in detail previously. The surface chemistry of CDC is investigated by temperature programmed desorption with mass spectrometry (TPD-MS) and energy dispersive X-ray spectroscopy (EDS). EDS provides information on the bulk atomic composition of CDC, while TPD-MS simultaneously detects multiple species desorbing from the surface of CDC upon heating. Analysis of TDP-MS spectra allows speculating on the nature of the surface functional groups, their thermal stability, and the presence of molecules trapped in pores. The porosity and specific surface area (SSA) are determined based on volumetric adsorption measure-

* Corresponding author. Tel.: +1 215 895 6446; fax: +1 215 895 1934.
E-mail address: gogotsi@drexel.edu (Y. Gogotsi).
[1] Current address: Department of Materials Science and Engineering, Massachusetts Institute of Technology, Cambridge, MA 02139, USA.

0040-6031/$ – see front matter © 2009 Elsevier B.V. All rights reserved.
doi:10.1016/j.tca.2009.09.002

ments. Structural ordering of as-produced and post-treated CDC is probed by Raman spectroscopy.

2. Experimental

2.1. CDC synthesis

The CDC synthesis has been described in detail elsewhere [10]. TiC with a particle size ranging from 2 to 4 μm (Atlantic Equipment Engineers; 99.9% purity) was used as a precursor. The powder was placed in a quartz tube and heated to either 600, 800 or 1100 °C in a furnace under Ar flow. Then Ar flow was switched to Cl_2 and chlorination for 3 h at either 600, 800 or 1100 °C was used to extract Ti:

$$TiC(s) + 2Cl_2(g) \rightarrow TiCl_4(g) + C(s) \quad (1)$$

After chlorination, the powders were treated for 1.5 h at 600 °C in Ar, H_2 or NH_3 in order to remove chlorine and volatile metal chlorides from the pores. The post-treatments were performed at 600 °C, the lowest chlorination temperature used, to minimize changes introduced to the structure of CDC by post-treatment.

2.2. Characterization

The SSA and porosity of the CDCs were characterized using volumetric sorption measurements (Quadrasorb from Quantachrome Instruments) in N_2 at 77 K and CO_2 at 273 K. The SSA was calculated using Brunauer–Emmett–Teller (BET) analysis using N_2 sorption [11]. Pore volumes and pore size distributions (not shown) were determined using the non-local density functional theory (NLDFT) model [12] using software provided by the instrument package (QuadraWin), and assuming the pores have a slit shape.

The elemental composition of CDCs was probed by EDS using a FEI XL30 scanning electron microscope equipped with an EDAX detector at an accelerating voltage of 20 kV.

Raman spectroscopy was used to characterize the microstructure of the CDCs. Spectra were acquired using a Renishaw (UK) 1000/2000 Raman micro-spectrometer with an excitation wavelength of 514.5 nm (Ar ion laser).

Thermogravimetric analysis (TGA) was performed using a SDT 2960 DTA-TGA (TA instruments). Samples were heated from 25 to 700 °C at 2 °C/min under 40 ml/min air flow.

TPD-MS studies were performed in a high vacuum chamber ($<10^{-8}$ Torr) equipped with a residual gas analyzer (RGA 300, SRS) [13]. The CDC powder was directly pressed between two stainless steel blocks into a W-grid and a thermocouple was spot-welded to the W-grid. The sample was then placed into the vacuum chamber and pumped to $<10^{-8}$ Torr at room temperature. Before experiment the sample was cooled to −173 °C with liquid nitrogen. TPD-MS spectra were recorded in the 1–100 amu range while heating samples at 2 °C/s from −173 to 1127 °C (Fig. 1). Approximately 100 TPD-MS curves in 1–100 amu range were collected during a single run, corresponding to 1 data point for a given mass per 10 °C. For further analysis, profiles of masses of interest were extracted from the full TPD-MS spectrum and plotted as a function of temperature.

3. Results and discussion

The impact of the chlorination temperature on pore texture modification of TiC-CDC has been studied and described elsewhere [2,3]. Table 1 reports the modification of specific surface area (SSA) and pore volumes with annealing treatment. As compared to Ar annealed samples, the SSA and volumes of the H_2 and NH_3 annealed ones do not show major changes proving that the chlorination temperature might have more effect on pore texture modification than the annealing atmosphere. The SSA increases with increasing chlorination temperature from 600 to 800 °C, but then slightly decreases after chlorination at 1100 °C. The total pore volume increases with chlorination temperature, while the micropore volume decreases. Furthermore, it can be seen that the post-treatments also affect the SSA and pore volume; CDCs post-treated in H_2 and NH_3 exhibit a higher SSA and pore volume than CDCs post-treated in Ar (Table 1).

The amount of Ti, Cl, and O present in CDC was determined by EDS. Fig. 2 shows the amount of Cl present in CDC as a function of chlorination temperature and post-treatment. For Ar treated samples, the Cl content decreases with increasing synthesis temperature. CDCs treated in H_2 and NH_3 contain only small amounts of Cl (<1 wt.%). However, the post-treatment in NH_3 appears to be slightly more efficient for Cl removal than post-treatment in

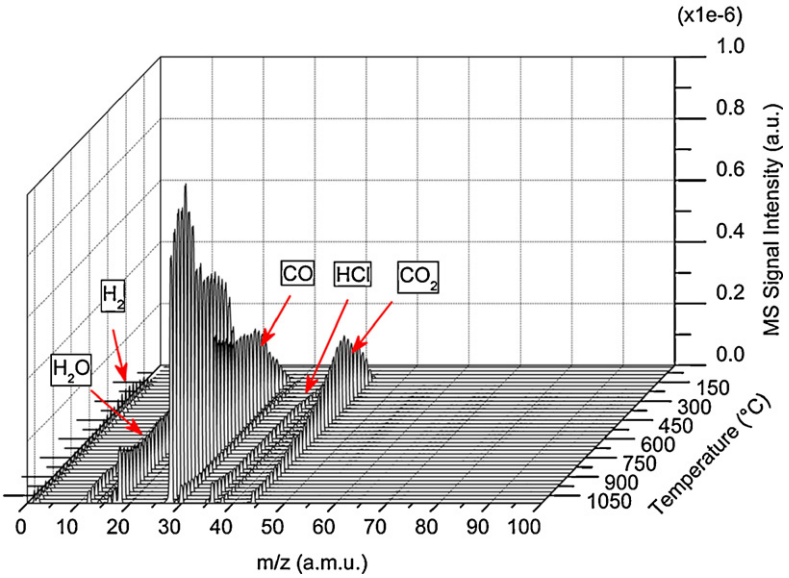

Fig. 1. Full TPD spectrum collected from CDC sample chlorinated at 600 °C and post-treated with Ar at 600 °C. The mass spectrometer detects all species in the 1–100 amu range while the temperature steadily increased from −173 to 1171 °C. Multiple peaks can be seen and are assigned to H_2, H_2O, CO, Cl, HCl, and CO_2.

Table 1
SSA, total pore volume and micropore volume of the CDCs produced at different temperatures and annealed in different gases at 600 °C.

Post-treatment conditions	BET SSA (m^2/g)	Pore volume, v_{N_2} (cm^3/g)	Micropore volume, v_{CO_2} (cm^3/g)	Volume of pores < 1 nm (cm^3/g)
600 °C, Ar	1290	0.48	0.44	0.35
600 °C, H_2	1365	0.51	0.46	0.38
600 °C, NH_3	1382	0.53	0.42	0.34
800 °C, Ar	1468	0.58	0.41	0.30
800 °C, H_2	1480	0.62	0.43	0.34
800 °C, NH_3	1556	0.65	0.42	0.32
1100 °C, Ar	1362	0.61	0.33	0.26
1100 °C, H_2	1368	0.68	0.24	0.19
1100 °C, NH_3	1330	0.71	0.29	0.22

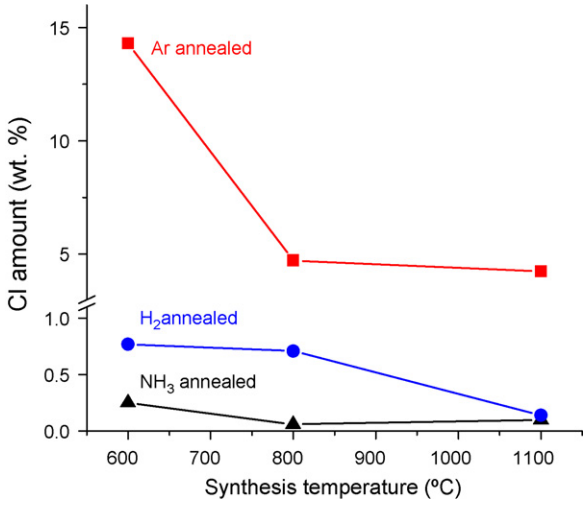

Fig. 2. Amount of residual Cl, determined by EDS, left in CDCs produced under different chlorination temperatures (600, 800, and 1100 °C) and post-treatment atmospheres (Ar, NH_3, and H_2).

H_2. The amount of Ti and O found in all CDC samples (data not shown) was about 0.3 and 7 wt.%, respectively, and did not show significant changes upon variations in chlorination temperature or post-treatment gases.

Raman spectra of TiC-CDC chlorinated at 600 and 800 °C annealed in Ar and NH_3 are shown in Fig. 3a. The post-treatment has no significant effect on the carbon microstructure. An increase in the chlorination temperature results in an increased ordering of the carbon, as indicated by the decreasing I_D/I_G ratio (Fig. 3b). The smaller I_D/I_G ratio obtained after NH_3 annealing suggests a more ordered structure as compared to the Ar annealed samples.

TGA experiments also show a difference between Ar and H_2/NH_3 treated samples chlorinated at 600 °C (Fig. 4). Between 100 and 250 °C, a weight loss of ~20% is observed for the Ar post-treated CDC, presumably corresponding to chlorine containing species (e.g., HCl) and/or H_2O desorption that were observed in TPD spectra for Ar post-treated CDC (Figs. 5a and 6a). The oxidation of CDCs starts around 450 °C and the same oxidation rate is observed independent of the annealing treatment. A slight increase in the oxidation temperature is observed for the H_2 post-treated CDC which can be explained by its more ordered structure (Fig. 3) [14,15].

TPD-MS experiments revealed variations in amount of Cl species desorbing from CDCs pretreated differently (Fig. 5). The only sample that showed significant desorption of Cl species was TiC-CDC chlorinated at 600 °C and post-treated in Ar (Fig. 5a). The release of HCl from CDC samples post-treated in Ar at 600 °C can be explained by formation of chlorine containing complexes that do not decompose (volatilize) at 600 °C (e.g., surface TiCl). After exposure of samples to ambient air, those complexes can be hydrolysed with formation of HCl and surface hydroxides (TiOH). For all other samples, the TPD-MS results suggest no detectable signal of Cl-containing species. Thus, in the case of TiC-CDC chlorinated at 600 °C, post-treatments in reductive atmospheres, such as H_2 or NH_3, effectively remove Cl. The possible chemical mechanism of chlorine removal could be described by the following equations:

$$\frac{1}{2}H_2 + Cl_{surf} \rightarrow HCl \quad (2)$$

$$4NH_3 + 6Cl_{surf} \rightarrow 2NH_4Cl + N_2 + 4HCl \quad (3)$$

TiC-CDC synthesized at 1100 °C and annealed in Ar shows desorption of Cl-containing species of at least two orders of magnitude lower than TiC-CDC produced at 600 °C (Fig. 5a and b). For samples chlorinated at 800 and 1100 °C and post-treated in Ar, the absence of Cl-containing species leaving the surface upon heating can be explained by a more effective diffusion of weakly bonded Cl in larger pores (Table 1) allowing a faster and more complete removal of Cl during synthesis [9]. Also, some of the Cl could bind chemically to the carbon surface [9,16], requiring significantly higher

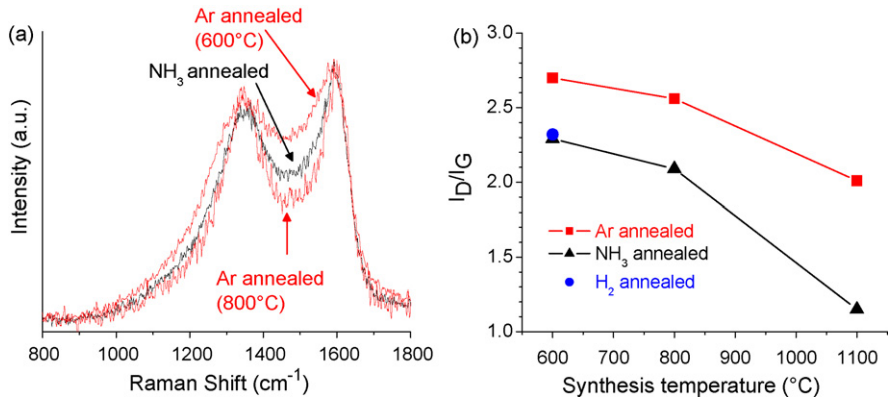

Fig. 3. Raman spectra of the CDC synthesized at 600 and 800 °C annealed in Ar and NH_3 at 600 °C (a). Variation of the I_D/I_G ratio as a function of chlorination temperature (b).

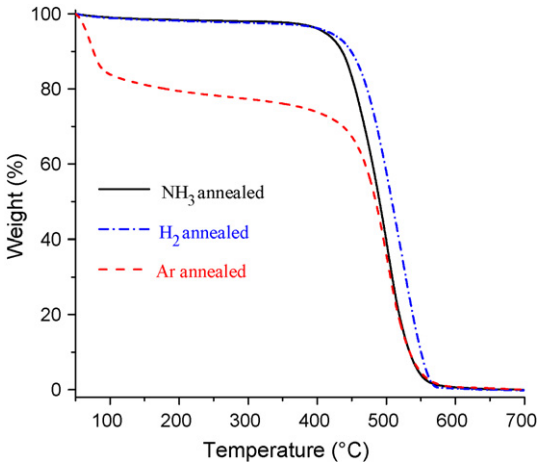

Fig. 4. TGA of CDCs synthesized at 600 °C, annealed in Ar, H_2 and NH_3. Heating rate 2 °C/min.

temperatures for Cl removal. Papirer et al. reported Cl bonded to carbon blacks in the form of CCl, CCl_2 and CCl_3 groups, which had a strong effect on surface properties by exhibiting a greater hydrophobic behavior [9,17,18]. It has been demonstrated that covalently bonded Cl cannot be removed completely by heating to 1200 °C [16]; by analogy we think that Cl remains on the surface of CDC even at higher temperatures. This is consistent with our experimental observations where only small quantities of desorbing Cl were detected by TPD-MS for samples chlorinated at 800 and 1100 °C (Fig. 5), even though Cl was detected by EDS for the same samples (Fig. 2). TPD-MS detects functionalities that desorb in the temperature range explored (−173 to 1127 °C), while EDS detects all the species present in the sample even those that do not desorb upon heating. To summarize, the results of both TPD-MS and EDS suggest that H_2 and NH_3 post-treatments remove residual Cl more effectively than post-treatments in Ar.

Along with chlorine, water is released during CDC heating (Fig. 1). Moisture sorption from air is important, because it can strongly affect performance of the carbon sorbent. In addition, moisture removal is arguably the most important step in the preparation of supercapacitor electrodes. H_2O (18 amu) desorption profiles were compared for samples subjected to different pretreatment procedures in order to address the question of CDC affinity for water (Fig. 6). Samples chlorinated at 600 °C, display similar H_2O desorption profiles independent of the post-treatment. As an example, the H_2O desorption profile for TiC-CDC chlorinated at 600 °C and post-treated in Ar is shown in Fig. 6a. The amount of H_2O desorbing at ~300 °C significantly exceeds the amount of water released above 800 °C (Fig. 6a). The signal observed at higher temperatures most likely originates from the decomposition of OH-containing functionalities on the carbon surface.

The decrease in the amount of H_2O desorbed with increasing chlorination temperatures (Fig. 6b and c) can be explained by increased ordering of CDC with temperature (Fig. 3) and decreased density of functional groups, that are responsible for wetting of carbon surface. This is consistent with results discussed below (Fig. 7); the higher the chlorination temperature the fewer oxygen-containing functionalities are found.

To summarize, we found that samples chlorinated at 600 °C and exposed to ambient air retain a significant amount of water that desorbs with maximum rate at 300–500 °C, while samples chlorinated at 800 and 1100 °C retain less water. Thus, the chlorination temperature is the prime factor that defines sample affinity to H_2O. This may be explained by increased graphitic ordering that makes CDCs less reactive towards ambient species (O_2 and H_2O) that can form hydrophilic oxygen-containing functionalities.

Analysis of the desorption profiles of CO (28 amu) and CO_2 (44 amu) shows that both species desorb from all CDC samples, suggesting the presence of oxygen functionalities. It can be seen that TPD-MS profiles of CO and CO_2 (Fig. 7) desorbing from both CDC (Cl_2 600 °C, Ar 600 °C) do not follow the H_2O desorption profiles (Fig. 6). The lack of correlation between desorbing H_2O, and CO or CO_2 can be explained by independent processes: water desorption from pores, surface dehydroxylation, and decomposition of surface functionalities (carbonyl, carboxyl, and other groups).

It is well known that CO and CO_2 can form upon decomposition of acidic and anhydride groups at temperatures ~200–600 °C [19,20], while CO desorbing at >600 °C can originate from decom-

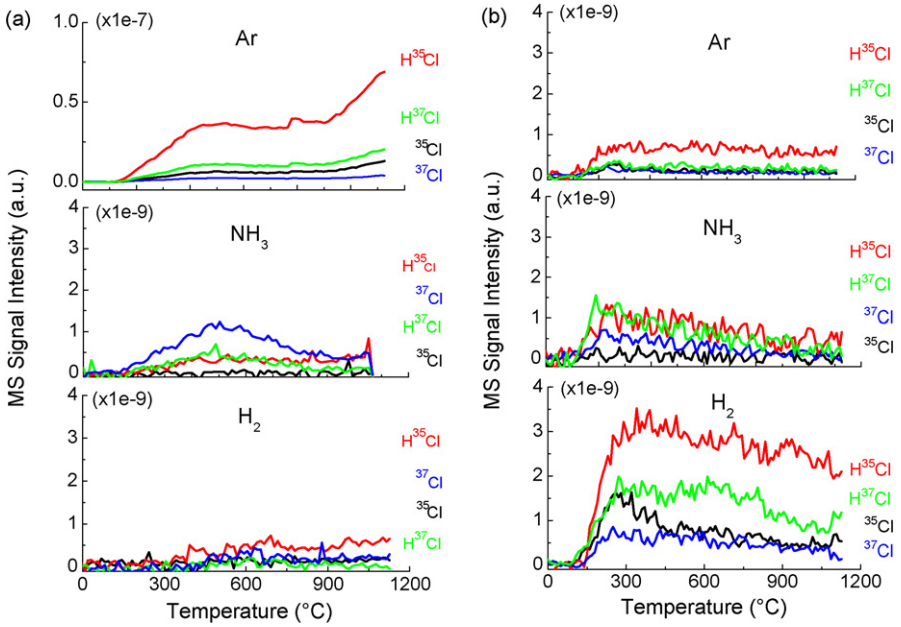

Fig. 5. TPD profiles of HCl and Cl evolved from CDCs chlorinated at 600 °C (a) and 1100 °C (b) and post-treated in Ar, NH_3 and H_2. Except for the 600 °C CDC annealed in Ar, there is no conservation of ratios characteristic to natural ^{35}Cl and ^{37}Cl (3:1) abundance suggesting limited desorption of Cl and HCl (note the difference in scale for Ar-600 °C sample).

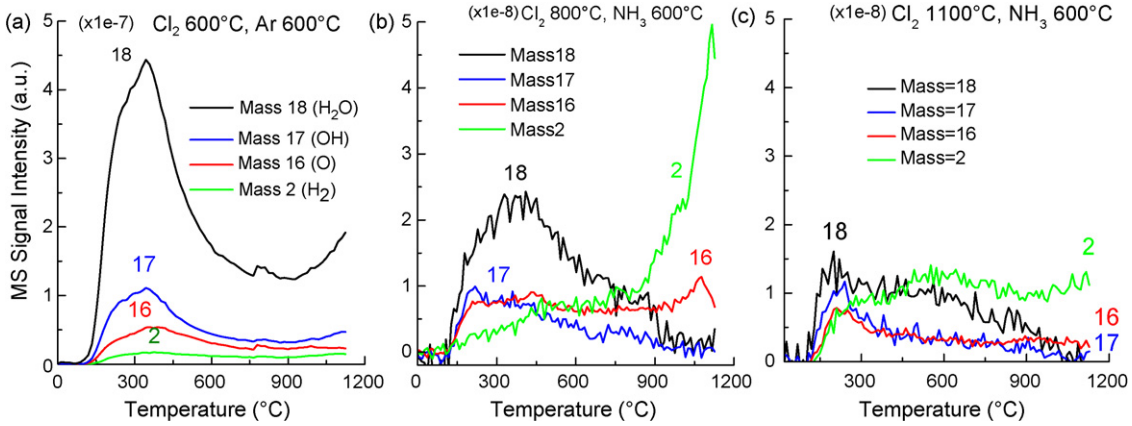

Fig. 6. H_2O desorption profiles from CDCs synthesized at 600 °C and post-treated under Ar (a), CDCs synthesized at 800 °C (b) and 1100 °C (c) post-treated under NH_3. The amount of H_2O that can be retained by CDC depends on chlorination temperature: the higher the chlorination temperature the lower is the amount of H_2O that can be retained.

position of neutral and basic groups [19,20]. For the 600 °C series, the CO and CO_2 profiles indicate that the post-treatment has no significant impact on the nature and amount of oxygen-containing functional groups (Fig. 6a and b). The CO_2 desorption profile shows a broad peak between 150 and 600 °C that is likely a result of the decomposition of carboxylic, anhydride and lactone groups [19,21,22]. CO that evolves above 600 °C can be assigned to the decomposition of phenol, carbonyl, and quinone groups [22–24]. Because of broad and overlapping profiles of desorbing species the unambiguous assignment of the observed TPD-MS peaks to certain functionalities is a challenging task. The main conclusion that follows from our TPD-MS investigation is the presence of oxygen functionalities at the surface of CDC. Those results were confirmed by FTIR. However, quantitative FTIR analysis of oxygen functionalities in CDC was difficult due to low transparency of CDC and necessity to dilute CDC with KBr or other salts.

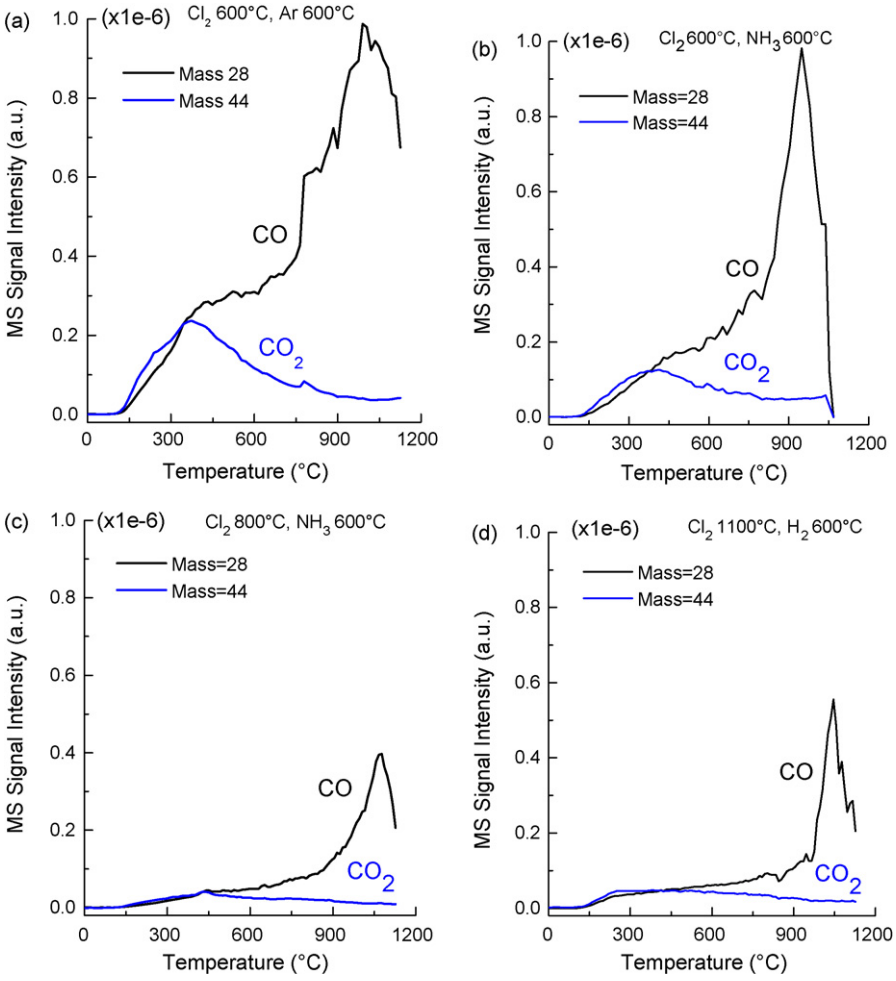

Fig. 7. CO and CO_2 profiles of the 600 °C CDC post-treated under Ar (a) and NH_3 (b) and 800 °C CDC post-treated under NH_3 (c) and 1100 °C CDC post-treated under H_2 (d).

In general, while there was no effect of post-treatment on the amount or nature of oxygen functionalities, the increase in chlorination temperature resulted in decrease of intensity of both CO and CO_2 evolving from CDC samples. The CO_2 desorption profiles for the samples chlorinated at 800 and 1100 °C are broadened and the maxima are not centered around 300 °C (Fig. 6b and c) as for samples chlorinated at 600 °C (Fig. 6a and b). The peak of CO desorbing at ~1000 °C becomes narrower and shifts to higher temperatures for samples chlorinated at 800 and 1100 °C (Fig. 6b and c). The change in CO desorption profiles indicates a modification of the type of oxygen functionalities [22,23].

According to our experimental data, the formation of oxygen surface moieties occurs after exposure of CDC samples to ambient air. The TiC precursor has <2% of oxygen. Moreover, most of the oxygen-containing surface functionalities [19,20] cannot survive the temperatures used during CDC synthesis (≥600 °C).

Both chlorination and post-treatment procedures exclude contact of CDC with oxygen and/or H_2O during the synthesis. Thus, the only possibility for oxygen functionalities introduction to CDC is the contact of freshly synthesized CDC with ambient air at room temperature. Zhuang et al. reported the formation of oxygen-containing functional groups on the surface of carbon after exposure to air, suggesting a chemical interaction with O_2 and/or H_2O [25,26]. Overall, the post-treatments have a minor effect on the formation of oxygenated functional groups, while it seems that chlorination temperature is the main factor responsible for reactivity of CDC with respect to ambient species (oxygen and water).

We believe that the reactivity of the CDCs with respect to oxygen and water, and the nature of oxygen functionalities, depends mainly, but not exclusively, on the ordering of CDC. As CDC chlorinated at 600 °C have a less ordered structure compared to the ones synthesized at higher temperatures (Fig. 4), the CDC with higher order are likely to be less reactive towards atmospheric species forming less oxygen functionalities. The information obtained from TPD-MS is not enough to assign the present surface oxygen functionalities based on desorption temperature. Other experimental techniques (e.g., Boehm titration) must be involved to identify the nature of the groups [27–29].

4. Conclusions

A correlation between the synthesis conditions, structure and surface chemistry of CDC was established. Increase of chlorination temperature results in higher mesoporosity of CDCs, while microporosity decreases. Post-treatment does not have significant impact on CDC porosity. The ordering (graphitic character) of the CDC increases with increasing the chlorination temperature. It results in a lower reactivity of CDC with respect to ambient species. The study of the influence of post-treatment under Ar, H_2 and NH_3 of TiC-CDC synthesized at different temperatures has shown that the residual chlorine content can be reduced significantly in reductive atmosphere of NH_3 or H_2. On the contrary, post-treatment under Ar for samples chlorinated at 600 °C leaves significant amount of chlorine.

Samples chlorinated at 600 °C are more reactive towards atmospheric species, leading to increased formation of oxygen functionalities and increased hydrophilicity in comparison with samples chlorinated at higher temperatures (800 and 1100 °C).

Acknowledgements

We are thankful to Professor Christopher Li (Drexel University) for providing access to the TGA and Professor J.E. Fischer (University of Pennsylvania) for helpful discussions. SEM and Raman spectrometer were provided by Centralized Research Facilities of Drexel University. The authors are grateful to the US Department of Energy (DOE), EERE Program, grant number DE-FC36-04GO14282, as well as to DOE's Office of Basic Energy Sciences, for financial support for this research.

References

[1] F. Schuth, K. Sing, J. Weitkamp, in: F. Schuth, K.S.W. Sing, J. Weitkamp (Eds.), Handbook of Porous Solids, Wiley-VCH, 2002, pp. 1766–1960.
[2] R. Dash, J. Chmiola, G. Yushin, Y. Gogotsi, G. Laudisio, J. Singer, et al., Titanium carbide derived nanoporous carbon for energy-related applications, Carbon 44 (2006) 2489–2497.
[3] J. Chmiola, G. Yushin, Y. Gogotsi, C. Portet, P. Simon, P.L. Taberna, Anomalous increase in carbon capacitance at pore sizes less than 1 nanometer, Science 313 (2006) 1760–1763.
[4] G. Yushin, A. Nikitin, Y. Gogotsi, Carbide-derived carbon, in: Nanomaterials Handbook, 2006, pp. 239–282.
[5] Y. Gogotsi, S. Welz, D.A. Ersoy, M.J. McNallan, Conversion of silicon carbide to crystalline diamond-structured carbon at ambient pressure, Nature 411 (2001) 283–287.
[6] E. Frackowiak, F. Beguin, Electrochemical storage of energy in carbon nanotubes and nanostructured carbons, Carbon 40 (2002) 1775–1787.
[7] F.L. Darkrim, P. Malbrunot, G.P. Tartaglia, Review of hydrogen storage by adsorption in carbon nanotubes, Int. J. Hydrogen Energy 27 (2002) 193–202.
[8] S.S. Barton, M.J.B. Evans, J.E. Koresh, H. Tobias, The effect of chlorination on the adsorptive properties of water on carbon cloth, Carbon 25 (1987) 663–667.
[9] E. Papirer, R. Lacroix, J.-B. Donnet, G. Nanse, P. Fioux, XPS study of the halogenation of carbon black. Part 2. Chlorination, Carbon 33 (1995) 63–72.
[10] R.K. Dash, A. Nikitin, Y. Gogotsi, Microporous carbon derived from boron carbide, Micropor. Mesopor. Mater. 72 (2004) 203–208.
[11] S. Brunauer, P. Emmett, E. Teller, Adsorption of gases in multimolecular layers, J. Am. Chem. Soc. 60 (1938) 309–319.
[12] P.I. Ravikovitch, A.V. Neimark, Characterization of nanoporous materials from adsorption and desorption isotherms, Colloids Surf. A 187–188 (2001) 11–21.
[13] S. Kwon, R. Vidic, E. Borguet, The effect of surface chemical functional groups on the adsorption and desorption of a polar molecule, acetone, from a model carbonaceous surface, graphite, Surf. Sci. 522 (2003) 17–26.
[14] H. Nakazawa, T. Kawabata, M. Kudo, M. Mashita, Structural changes of diamond-like carbon films due to atomic hydrogen exposure during annealing, Appl. Surf. Sci. 253 (2007) 4188–4196.
[15] N.M.J. Conway, A.C. Ferrari, A.J. Flewitt, J. Robertson, W.I. Milne, A. Tagliaferro, et al., Defect and disorder reduction by annealing in hydrogenated tetrahedral amorphous carbon, Diamond Relat. Mater. 9 (2000) 765–770.
[16] B.R. Puri, R.C. Bansal, Surface chemistry of carbon blacks. IV. Interaction of carbon blacks with gaseous chlorine, Carbon 5 (1967) 189–194.
[17] C.R. Hall, R.J. Holmes, The preparation and properties of some activated carbons modified by treatment with phosgene or chlorine, Carbon 30 (1992) 173–176.
[18] C.R. Hall, R.J. Holmes, The preparation and properties of some chlorinated activated carbons. Part II. Further observations, Carbon 31 (1993) 881–886.
[19] J.L. Figueiredo, M.F.R. Pereira, M.M.A. Freitas, J.J.M. Orfao, Modification of the surface chemistry of activated carbons, Carbon 37 (1999) 1379–1389.
[20] A.E. Aksoylu, M. Madalena, A. Freitas, M.F.R. Pereira, J.L. Figueiredo, The effects of different activated carbon supports and support modifications on the properties of Pt/AC catalysts, Carbon 39 (2001) 175–185.
[21] Y. Otake, R.G. Jenkins, Characterization of oxygen-containing surface complexes created on a microporous carbon by air and nitric acid treatment, Carbon 31 (1993) 109–121.
[22] U. Zielke, K.J. Huttinger, W.P. Hoffman, Surface-oxidized carbon fibers. I. Surface structure and chemistry, Carbon 34 (1996) 983–998.
[23] J.L. Figueiredo, M.F.R. Pereira, M.M.A. Freitas, J.J.M. Orfao, Characterization of active sites on carbon catalysts, Ind. Eng. Chem. Res. 46 (2007) 4110–4115.
[24] B. Marchon, J. Carrazza, H. Heinemann, G.A. Somorjai, TPD and XPS studies of O_2, CO_2, and H_2O adsorption on clean polycrystalline graphite, Carbon 26 (1988) 507–514.
[25] Q.L. Zhuang, T. Kyotani, A. Tomita, The change of TPD pattern of O_2-gasified carbon upon air exposure, Carbon 32 (1994) 539–540.
[26] Z.R. Yue, W. Jiang, L. Wang, S.D. Gardner, J.C.U. Pittman, Surface characterization of electrochemically oxidized carbon fibers, Carbon 37 (1999) 1785–1796.
[27] J.-H. Zhou, Z.-J. Sui, J. Zhu, P. Li, D. Chen, Y.-C. Dai, et al., Characterization of surface oxygen complexes on carbon nanofibers by TPD, XPS and FT-IR, Carbon 45 (2007) 785–796.
[28] H.P. Boehm, Surface oxides on carbon and their analysis: a critical assessment, Carbon 40 (2002) 145–149.
[29] X. Feng, N. Dementev, W. Feng, R. Vidic, E. Borguet, Detection of low concentration oxygen containing functional groups on activated carbon fiber surfaces through fluorescent labeling, Carbon 44 (2006) 1203–1209.